An assessment of eddy viscosity models on predicting performance parameters of valves

Yu Duan[1*], Christopher Jackson[2], Matthew D. Eaton[1], Michael J. Bluck[1]

1. Department of Mechanical Engineering, Imperial College London, London, UK

2. SMRs R&T Modelling & Analysis, Rolls-Royce, Derby, UK

Abstract

The major objective of the present study is to evaluate the performance of a range of turbulent eddy viscosity models in the prediction of macro-parameters (flow coefficient (C_Q) and force coefficient (C_F)), for certain types of valve, including the conic valve, the disk valves, and the compensated valve. This has been achieved by comparison of numerical predictions with experimental measurements available in the literature. The examined turbulence models include most of the available turbulent eddy viscosity models in STAR-CCM+ 12.04. They are the standard k-ε model, realizable k-ε model, k-ω-sst model, V2F model, EB k-ε model and the Lag EB k-ε models.

The low-Re turbulence models (k-ω-sst, V2F, EB k-ε and Lag EB k-ε) perform worse than the high-Re models (standard k-ε and realizable k-ε). For the conic valve, the performance of different turbulent models varies little; the standard k-ε model shows a marginal advantage over the others. The performance of the turbulence models changed greatly, however, for prediction of C_Q and C_F of the disk and compensated valves. In general, the realizable k-ε model is demonstrated to be a robust choice for both valve types. Although the EB k-ε may marginally outperform it in the prediction of C_F at large disk valve opening.

The effects of the unknown entry flow and initialization conditions are also studied. The predictions are more sensitive to the entry flow condition when the valve opening is large. Additionally, the uncertainties caused by unknown entry conditions are comparable to overall modelling errors in some cases. For flow systems with multiple stable flow-states coexisting in the flow domain, the output of the numerical models can also be affected by the initialization conditions.

When the streamline curvature and secondary flow is modest like conical valve flow, the nonlinear modification of the standard k-ε model and k-ω-sst model, as well as the curvature correction in the realizable k-ε model, will not have visible effects on the numerical prediction. Once the strong streamline curvature and secondary flow exit in the domain, such as the disk valve flow, the non-linear modification of the standard k-ε model will greatly improve the numerical outputs, however, the non-linear modifications of k-ω-sst model only have minor effects. Moreover, the curvature correction in the realizable k-ε model will jeopardise the accuracy of outputs in the same case.

Keywords: Valve; Complex flow; Computational Fluid Dynamics (CFD); Reynolds-Averaged Naiver-Stokes (RANS); Turbulence models

Introduction

---

* Corresponding author. Email: y.duan@imperial.ac.uk

Valves are amongst the most common and valuable components in power plants. Typically, there are approximately 4000 valves in a fossil fuel power plant, and the number can be ten times larger in a nuclear power station. As a consequence, the performance of valves attracts considerable attention from both industry and academia. Internal flow behaviours in a valve, usually very complex, are strongly dependent on the valve design, working fluid properties, and operating conditions. Flow separations, reattachments, recirculation, shockwaves and shock-boundary interactions may coexist in the valve during operation. In subsonic valves, the former three flow topologies are expected to dominate the domain. Once the fluid velocity through the throttle matches the sonic level, as in pressure relief valves, shockwaves will be formed. Subsequently, the flow will be choked, and shock-boundary-layer interaction may be triggered. If the working fluid is liquid, such as water, cavitation/flashing will occur once the pressure drop is sufficient.

Traditionally, the performance of a valve design is examined by physical testing. However, building experimental facilities is normally expensive and time-consuming. Thanks to advances in the computational fluid dynamics (CFD) methodology, in tandem with the exponential growth of computing power, CFD has become a feasible alternative. Extensive CFD studies of valve flows have been conducted in support of understanding and improving designs. Some examples of such CFD studies can be found in [1-14]. Similar to experimental measurements, there are uncertainties/errors in all of the industrially practical CFD methods. In addition to the user errors, other errors in a simulation are normally due to three factors: parametric errors, numerical discretisation errors (.e.g. spatial mesh size and temporal resolution) and modelling errors. The most significant of these is modelling error due to oversimplifications of flow phenomena in the mathematical model, followed by numerical discretisation error which is largely due to insufficient mesh resolution, and then parametric errors due to lack of detailed knowledge of the geometry and fluid properties. In terms of valve flow, the oversimplification of the flow phenomena in a CFD model can be due to the turbulence models used in the RANS method and a lack of adequate representation of cavitation when it happens [15]. The well-known cavitation models, such as the Rayleigh-Plesset model and the Schnerr-Sauer model, rely on the predicted static pressure domain to provide the likelihood of cavitation [16]. As a result, the predicted flow domain is the key to capturing cavitation, in which case, the turbulence model plays an important role. The turbulence models are created based on the knowledge of the flow physics and the intuition of the model developers. It is not surprising that the accuracy diminishes as the model is applied to problems which deviate from the set of the calibration cases. It is important to validate the turbulence model before applying it to the complex flow systems.

Vaughn, Johnston & Edge [17] studied incompressible flows in various poppet valves. It was concluded in the article that the standard k-ε model performed well for a simple conic plug valve design, but experienced difficulties capturing the flow separation and recirculation in valves with more complex configurations, i.e. the disk/compensated plug. In the work by Huang & Kim [18] the same turbulence model and wall function were used to simulate water flow in a butterfly valve. The deviation between predicted pressure loss coefficient and experimental measurement increased as the valve closed. Similar results can also be found in Wallace et al. [19] and Song & Park [20]. Wallace et al. [19] reported the numerical simulations of flow in a choked valve. The turbulence effect was modelled by the standard k-ε model. In the latter article [20] the same turbulence model and wall treatment were applied to simulate water flow in a butterfly valve. In both articles, the predicted discharge coefficients of the valves at small openings were significantly different from measurements.

Conversely, good performance of the standard k-ε model was reported in [21], in which a 3D CFD model was applied to simulate water flow in a control valve. The model accurately predicted the pressure distributions. Differences between predicted local pressures and physical measurements were generally smaller than 6%.

In [22] and [23], Davis and Stewart examined the prediction of incompressible flow in globe control valves using the RNG k-ε model and standard wall treatments. A mismatch between experimental measurements and numerical simulations is again documented in the papers. The deviation was small when the valve opening was 10% but gradually increased for the larger openings. In their best scenario, the predicted discharge coefficient (C_v) almost overlapped with the measurement, at a small opening of one of the studied valves. In the worst case, the model overestimated the C_v by a factor of 2.

The Chen k-ε model was adopted by Moujaes and Jagan [24] to predict the pressure loss coefficient of a ball valve. The error of the predicted loss coefficients was within ±5%. Sibilla and Gallati [25] examined the capabilities of various versions of the k-ε turbulence models (standard k-ε, Chen k-ε and RNG k-ε) in predicting the pressure drop and flow coefficient of incompressible flow in a nozzle check valve. In terms of the flow coefficient at the fully opened stage, the value obtained using RNG k-ε was just 4% higher than measurements, while the standard and the Chen version were up to 42% and 10% higher, respectively.

In [26], Toro reported the difficulties of using the realizable k-ε model and two-layer wall treatment in predicting the flow coefficients of a butterfly valve. The errors in the predicted loss coefficients at various openings of the valve varied within a range of around ±40%. The worst predictions were observed when the angle of the valve disk was at 10º or 90º. The best match between numerical results and experimental results was observed when the disk angle was in the range of 40º to 50º. In this range, errors in the predicted values were <5%. Leutwyler and Dalton claimed in [27-28] that k-ω-sst is the optimal model in terms of predicting pressure distribution on the valve disk, in comparison with the Spalart-Allmaras model, the standard k-ε model, the RNG k-ε model, the standard k-ω model. The performance of the standard k-ε, standard k-ω, and k-ω-sst models in fully 3D analyses estimating the overall force on the disc in a small hydraulic seat valve was examined in [31]. The most convincing prediction was made by the k-ω-sst model with non-dimensional wall distance y^+=27.61, irrespective of the opening of the valve.

As recorded above, many authors have tried to address question about the suitability of the turbulence models on predicting various valve flows. Most of the studies focused on comparing the numerical results to an experiment but lack discussion about the effects of mesh configurations, initialization conditions and unknown entry flow development. All of these factors will introduce uncertainty to the output and therefore jeopardise the judgement of the performance of the turbulence model. According to the best knowledge of the authors, applications of some recently developed turbulence models, such as EB k-ε, Lag EB k-ε and V2F, on modelling valve flows are missing from literature. Their performance on predicting valve flows therefore needs to be examined.

As a part of a verification and validation project for Rolls-Royce's small modular reactor (SMR) programme, this paper focuses on validating the eddy viscous turbulence models and near wall flow treatments available in the STAR-CCM+ 12.04 [16]. Of course, we acknowledge the benefit of the Reynolds Stress models (RSMs) in terms of reproducing the anisotropic turbulence. Compared to eddy viscosity turbulence models, the RSMs contain

more equations. As a result, more resources are needed for each simulation. In addition, the RSMs show significant numerical stiffness. In our preliminary study, the simulation using the RSMs normally lead to intolerable numerical instability or divergent simulations. By recognizing these difficulties, using the RSM models in an industrial context can be a great challenge. To make our study more practical and useful to industry, we limited our focus on the eddy viscosity turbulence models. Dependent on the prerequisite assumptions, a turbulence model can only model the effects of a range of turbulent eddy scales [30]. The applicability of a given turbulence model is highly dependent on the flow features that need to be captured. Good performance of one turbulence model on a specific type of flow system does not mean the turbulence model can be applied to other cases with the same confidence. Subsequently, three different valve designs are considered in our study. Modelling results are examined by comparing with experimental measurements reported in [31]. The sensitivities of the numerical prediction to the unknown stage of development of the entry flow as well as different initialization conditions are also investigated.

Methodologies

Brief Descriptions of the Experiment by Johnston, Edge & Vaughan [31]

An experimental rig was used to investigate the performance parameters of different plug configurations for a poppet valve. A diagram of the valve assembly with a 45º conical valve plug can be found on the left of Figure 1. Other plug configurations considered, such as a disk valve plug and a 45º conical compensated valve plug, are shown on the right of Figure 1. These three designs can represent the general plug shapes in control valves and pressure relief valves. The diameter of the inlet pipe and chamber were 25.4 mm and 74 mm, respectively. The Reynolds number of the incoming water flow varied from 2,500 to 35,000. Non-cavitation condition was reported in the experiment. In addition, it is stated in the paper that the flow coefficient (C_Q) did not vary significantly over their considered Re range. Two valve parameters, the flow coefficient (C_Q) and the force coefficient (C_F), are used to examine the performance of the poppet valves. The definitions of both parameters are listed below:

$$C_Q = \frac{Q}{\left(a\sqrt{\frac{2\Delta p}{\rho}}\right)} \tag{1}$$

where Q (m^3/s) is the volumetric flow rate, ΔP (Pa) is the pressure drop across the valve, ρ (kg/m^3) is the density, and a (m^3) is the orifice area of the valve, which is defined as

$$a = \pi d_{in} Z sin(\theta)\left\{1 - \frac{Z}{2d_{in}}\sin(2\theta)\right\} \tag{2}$$

In Eqn. (2), the d_{in} is the diameter of the inlet pipe, Z is the lift of the plug and θ is the half-angle of poppet cone.

$$C_F = \frac{F}{(\Delta PA)} \tag{3}$$

As described in Eqn. (3), the force coefficient C_F, is the ratio between the force (F) acting on valve head and the static pressure force ΔPA, where ΔP is the pressure drop across the valve and A is the area of inlet pipe cross section. By this definition, the fluid force contributes to

opening the valve when $C_F > 1.0$, while it acts to close the valve when $C_F < 1.0$. It should be mentioned the error of the measured lift in the experiment is ± 0.02 mm. The accuracy of measured flow ratio is ± 0.002 L/s, while the measured pressure with an accuracy of approximated ± 0.005 bar.

Geometries and Boundary Conditions

Since the test rig configurations were axisymmetric, 2D axisymmetric CFD models are created to simulate water flowing in the poppet valves. Views of the simulated flow domain in the models for various plug designs are illustrated in Figure 2. It should be noted that the height of the lip on the compensated valve head and thickness of the disc valve head were not reported in the paper. As a result, their dimensions are scaled from [29]. The length of the inlet is specified as $5d_{in}$, while the length of the outlet chamber is treated as $10d_{out}$. The density and viscosity of water, which is treated as incompressible in the CFD models, are specified as 1000 kg/m^3 and 0.001 Pa·S, respectively. The Reynolds number is taken as 10,000 while the calculated inlet bulk velocity is 0.3739 m/s. For assessing the performance of CFD models the value, 0.3739 m/s, is fixed at the inlet uniformly. Meanwhile, the turbulence intensity and turbulent viscosity ratio are set as 0.01 and 10.0, respectively, at the inlet for the cases. In the study of the entry flow effects, the downstream flow field, including velocity distribution and turbulence quantities, are copied to the inlet. As the experiments were conducted at room temperature, uncertainties due to the unknown water properties are deemed to be insignificant in our study. The numerical results of flow discharge coefficients (C_Q) and force coefficients (C_F) of valves at various lifts are compared to the experimental measurements. Since the error bar were not included in the original article, the success or otherwise of the models will be judged on their ability to predict the overall trend and experimental values of C_Q and C_F.

Governing Equations and Turbulence Modelling

The flows in the CFD models are governed by the Reynolds-Averaged Navier-Stokes (RANS) equations; these are closed by turbulent eddy viscosity models. This paper compares the ability of a wide range of turbulent eddy viscosity models available in STAR-CCM+ 12.04, including:

- Standard k-ε
    - Standard wall function treatment
    - Two-layer wall treatment
    - Low Re model
- Realizable k-ε
    - Standard wall function treatment
    - Two-layer wall treatment
- V2F
- k-ω-sst
- EB k-ε
- Lag EB k-ε

In these models, the effects of turbulence on the mean flow are treated as a dynamic viscosity. They model the turbulent viscosity based on a number of different assumptions.

The standard k-ε model has been widely applied in industry. However, as the standard k-ε model is not able to adequately resolve the near wall flow, an extra near wall flow treatment is required. The most popular choice is the standard wall function. In STAR-CCM+ 12.04, the standard k-ε model can be modified to adopt a two-layer near wall flow treatment.

Another version of the standard k-ε model available in STAR-CCM+ is the standard low-Re k-ε model. The damping function in the standard low-Re k-ε model allows it to be applied to the viscous sublayer near the wall.

Differences between the standard and realizable k-ε model lie in the interpolation of ε. While ε is treated as a portion of k in the standard k-ε model, the equation for ε in the realizable model is derived from the transport equation of the turbulent vorticity. The model satisfies certain mathematical constraints on Reynolds stresses, consistent with the physics of turbulent flows. Similar to the standard k-ε model, extra functions are required to solve the near wall flow. The standard choice for the realizable k-ε model is also a two-layer near wall treatment. This model can be modified to deal with the standard wall function in the STAR-CCM+ 12.04.

V2F consists of three transport equations for the turbulent kinetic energy, k, the dissipation rate, ε, as well as a transport equation for turbulence intensity, V2, normal to the streamline. In addition, a Helmholtz type equation for the quantity *f* which models the pressure-strain term is also included in the model. Distinct from the standard and realizable k-ε models, the turbulent viscosity is evaluated by considering the squared velocity scale of V2 and the time scale of local turbulence, which enables the model to better simulate flow recirculation.

The k-ω-sst model combines the standard k-ω model and standard k-ε model by introducing a blending function. In the near wall region, the flow is solved by the standard k-ω model, which offers a robust and accurate viscous sublayer formulation and more accurate prediction of the boundary layer in separated flows, while the flow outside of the boundary layer is modelled by a high Re version of k-ε model. The V2F and k-ω-sst models are better able to solve for flow near the wall. However, the additional equations increase the numerical stiffness and models tend to overpredict the velocity in the logarithmic region.

The EB k-ε model tries to address the problem by introducing a blending parameter in V2 to the V2F model and source term modelling to provide a smooth transition between the viscous sublayer and log-layer. The EB k-ε model intends to provide more accurate predictions in comparison with the realizable k-ε model, especially in the near wall region and more stable simulations compared to k-ω-sst and V2F. In separated/unsteady flow regions, non-equilibrium effects result in a misalignment of the principal components of the stress and strain-rate tensor, which lead to the over-prediction of turbulent kinetic energy production by linear eddy viscosity models. The Lag EB k-ε model incorporates the angle between these components, which allows the model to simulate anisotropy, curvatures and rotation effects.

The turbulence models which allow the near wall flow to be resolved directly (standard Low-Re k-ε, EB k-ε, Lag EB k-ε, V2F & k-ω-sst), are referred to as low Re turbulence models in the following discussions, while the standard k-ε and realizable k-ε with standard wall function or two-layer near wall treatment are referred to as high Re turbulence models. Other than the standard version of the standard k-ε model and the k-ω-sst model, we also tested the

'Quadratic' and 'Cubic' nonlinear modifications of both models, as well as the curvature correction of the realizable k-ε model. The transport equations of the turbulent quantities of turbulence models can be found in [16].

Numerical Methods

The flow domains in valves are discretized by non-uniform structured meshes. A view of the mesh of the conical valve is presented in Figure 3. Before commencing the examination of the eddy viscosity models, a mesh sensitivity study was completed to identify the most suitable mesh configuration. Other than some meshes in the mesh sensitivity study, the near wall y^+ was generally ~1. Although the near wall mesh is too fine for the standard wall function, it has been proven in the preliminary study that the effect of such fine near wall meshes on the prediction of C_Q and C_F is insignificant. To reduce numerical errors, sets of equations for control volumes in the flow domain are converted to a linear system using 2nd order upwind discretization. The pressure and velocity are coupled using the SIMPLE algorithm. The residuals of each simulation are $< 10^{-9}$, whilst the monitored local pressure reached a steady state by the termination of the simulation.

Results and Discussions

Mesh Sensitivity Study

Various meshes were generated according to different configurations. The edges of the geometry are shown in Figure 4 and the number of nodes on each of these edges is listed in Table 1. The major differences between the meshes lie in the resolution around the plug, corners and near wall region; the mesh resolutions for the upstream inlet pipe and downstream chamber are similar. As shown in Table 1, the number of mesh elements at streamwise ('V2' + 'H2') around the valve head increases from 40 to 600 in Msh-1 to Msh-4, while the number of grids allocated at the wall normal direction ('V1') is 10. Subsequently, the mesh quality reduces as the aspect ratios rise from Msh-1 to Msh-4. In Msh-5, the number of mesh elements in the wall normal direction is aggressively increased to 60 while the streamwise mesh resolution remains at 600. The wall normal mesh resolution is gradually decreased to 30 in the following three mesh configurations (Msh-6 to Msh-8). Since the allocation of grids across the streamwise direction in these three configurations is not changed, the aspect ratio is again spoiled. The number of grids at 'V2' and 'H2' are reduced to 40 and 30 respectively in Msh-9, to improve the mesh quality, namely the aspect ratios. It also should be noted that Msh-5a & 9a are configurations with refined mesh resolutions near walls and corners, whereby, the y^+ values are improved, in comparison with Msh-5 & 9. The maximum values of y^+ of the meshes are presented in Table 2. Most of the first nodes near the wall are allocated in the inner boundary layer except some in the chamber and on the front surface of the valve head. Refinements near the wall in Msh-5a and Msh-9a ensures that y^+ is around 1 or smaller. To reduce numerical errors and maintain numerical stability, sets of equations for control volumes in the flow domain are converted to a linear system using the 2nd order upwind discretization. The pressure and velocity are coupled using the SIMPLE algorithms.

Figure 5 shows C_Q for the conical valve at a lift of 2.54 mm obtained by the experiments [31] and predicted by the CFD models. The physical measurement is indicated by a dashed line in

the figure. In these models, the turbulence effect is modelled using various turbulence models considered in this study. In terms of near wall flow modelling method, the high y^+ wall treatment is applied in the CFD model with the standard k-ε model, two-layer near wall treatment is for the case using realizable k-ε model and all y+ wall treatment works with all the low-Re turbulence models. The mesh resolution, mesh quality and allocation of the mesh elements are factors which can affect the simulation accuracy. No matter what turbulence model was employed in the simulation, the mesh effect on the C_Q is similar. The overprediction gradually becomes more significant for the first four meshes. As the turbulence model is the same, the reason for the worsening predictions must be insufficient mesh resolution normal to the wall direction and a distorted mesh due to the aggressively increased number of mesh grids in the streamwise direction. The fidelity of the model is greatly improved (error <1%) when Msh-5 is used. The simulation error increases when the grids in the wall normal direction are decreased (see results of model adopting Msh-6, 7 & 8), which also leads to higher aspect ratios. The error is reduced again when Msh-9 is used. This is because the quality of the mesh in terms of aspect ratio is improved by removing some nodes at streamwise in the vicinity of the valve head. In addition, for a chosen turbulence model, the error in the simulation using Msh-5 and Msh-9 is very similar, which indicates the convergent of numerical error. Furthermore, it is worth to pointed out that the distorted meshes, Msh-6, 7 & 8, causes the divergent simulation or the significant numerical instability when the low-Re turbulence model is used in the CFD model, expect for V2F k-ε with Msh-7 & 8. Even in the case of using V2F k-ε with Msh-7 & 8, the under-relaxation factor has to be used. Hereby, much more iterations are required in order to make the simulation converge. This again indicates that the low-Re turbulence models are numerically stiffer than the high-Re turbulence models in general. In addition, the improved near wall and corner resolutions (Msh-5a and 9a) have some marginal effects on the accuracy of predictions. Considering the mesh requirements of turbulence models, especially low-Re turbulence models, Msh-9a is used to compare the capabilities of the turbulence models and wall treatments.

The Conic Valve

The performance of the different eddy viscosity models on predicting flow coefficient (C_Q) and force coefficient (C_F) are discussed in this section. There are three principal types of flow patterns reported in [31] for conic valves:

I. The jet flow follows the face of the conical plug until it meets the side wall
II. the jet flow reattaches to the valve seat
III. the jet flow passage bends toward the spindle

Type (III) flows are more likely to happen in small angle (<45º) conic valves. For the valve studied, the jet was commonly found to be stable for more than one flow pattern. In fact, the jet direction is historically dependent. Although we are only considering the prediction of a 45º conic valve, it is worth mentioning that for a 30º conic valve, C_F was highly dependent on the flow pattern while C_Q was not, refers to [31]. In this regard, the errors in the prediction of C_F, using RANS models, may be larger than that of C_Q, as the steady-state CFD model can only capture a single flow state, while in reality others co-exist.

Numerical results of C_Q and C_F and their physical measurements are compared in Figures 6 & 7. Irrespective of the turbulence modelling adopted, the predicted tendency of C_Q and C_F

follows the experimental observations. C_Q increases as a result of the valve opening, and C_F reduces. In terms of C_Q, the errors due to the different turbulence models are generally within ±5%. The standard k-ε model with the standard wall function is most accurate. The maximum difference between C_Q prediction and experimental measurements occurs for the standard low-Re k-ε model, whilst the predictions by the standard k-ε model with either of the standard wall or two-layer wall treatment almost overlap with each other. Similar observations can be made with the group of realizable k-ε models (with standard wall function/two-layer wall treatments). It is worth mentioning that the realizable k-ε model performs better with the standard wall function in terms of numerical stability.

Similar performance of the eddy viscosity models is also seen for the prediction of C_F, shown in Figure 7. Another feature shown in Figure 7 is that the low-Re turbulence models differ more from the measured C_F, such as the predictions by the V2F and k-ω-sst models. Also, for each turbulence model, the error in C_F increases with the valve opening, whilst that for the C_Q decreases. An example is at Z/d0 = 0.14. The errors for C_Q at this opening, computed by different models, are within ±1%, while the errors for C_F vary from 5% to -20%. This indicates that low-Re models have some difficulties in predicting the pressure on the valve head, although the predicted general pressure drop agrees well with the experiment.

The unknown condition of the entry flow may contribute to some extent to modelling errors. The sensitivity due to the various entry velocity conditions is examined using the realizable k-ε model with the two-layer wall treatment with five different velocity profiles, 'Inlet-01' to 'Inlet-05', which present flows of different stages of development in a pipe from a uniform distribution to a fully developed flow, illustrated in Figure 8. The variation is evaluated according to:

$$\frac{\left(C_i - mean(C_i)\right)}{mean(C_i)} \times 100\%$$

where C_i is the valve parameter (C_F or C_Q) with 'Inlet-i' as the inlet flow profiles at different flow development stages, i = 1, 2,.., 5. As shown in the figure, the uncertainty due to the different flow development stage is larger when the valve lift was higher. However, the sensitivity for both C_Q and C_F is, overall, less than 1%. Note that the small value of sensitivity does not necessarily mean less impact on the simulation accuracy. Taking the C_Q at Z/d0 ≈ 0.1 as an example, the sensitivity to the considered inlet flow profiles is about ±0.6%, which is comparable to the overall modelling error (~ -1%).

The Disk Valve

The flow pattern in disk valves differs from the conic valve. According to [31], when the opening is small enough, the jet from the throttle reattached to the seat within the clearance region and the pressure recovered significantly. As a result, C_Q was close to unity in the small opening range. As long as this flow pattern perseveres, C_Q increases with the valve opening. When the opening process continues, the separation bubble on the valve seat grows and stretches out within the clearance between the plug and valve seat. This causes the pressure loss to increase and C_Q decreases. The jet detaches from the valve seat once the opening is sufficiently large. In this type of design, the change occurred when the opening approached Z/d0 ≈ 0.07. C_Q slowly recovers after this point due to the larger clearance. When Z/d0 < 0.07 the force on the valve head assists the closure of the valve (C_F < 1.0), while the opposite

effect occurs once Z/d0 > 0.07. As with C_Q, a non-linear relationship between C_F and Z/d0 exists in the small opening range. For small openings, the jet is contracted by the separation bubble. The jet is further contracted when the opening is sufficiently small, whereby static pressure around the valve head is converted to dynamic pressure, which leads to a further reduction of the fluid force in the valve opening direction. Further opening results in a larger orifice area and vena contracta moving radially outward leading to pressure recovery near the plug, creating a stronger force.

As mentioned above, C_Q and C_F are highly dependent on the flow pattern. Therefore successful prediction is dependent on the success of the flow structure reconstruction.

Before continuing the discussion of the predicted valve performance parameters, it is worthwhile considering the flow field predicted around the plug by the turbulence models. The predicted flow pattern in the clearance formed by the disk and the valve seat at three levels, Z/d0 = 0.025, 0.05, 0.1, are included in Figures 9, 10 and 11. Since different versions of the standard k-ε model/realizable k-ε model produce almost identical flow patterns, we only include the prediction by their standard form in the figures. Overall, the turbulence models are able to reproduce the separation of the jet from the valve seat. However, the size of the separation bubble varies. The largest separation bubble is produced by the low-Re eddy viscosity models, except the standard low-Re k-ε model, while the smallest separation bubble was produced by the standard k-ε model. When Z/d0 = 0.01, the flow indicated by the realizable k-ε model is very similar to the prediction by other low-Re turbulence models.

The C_Q and C_F computed by the CFD models with different eddy viscosity models are compared with experimental measurements in Figures 12 and 13 The underestimation of flow separation in the vicinity of the valve plug by the standard k-ε model leads to very poor prediction of C_Q, and is a strong indication that standard k-ε models are to be avoided in these circumstances. The shapes of the C_Q profile produced by the other turbulence models are similar to each other and to the experimental results. For these models, the largest error is exhibited for the smallest openings. Generally, the smallest errors are obtained with the realizable k-ε models. The realizable k-ε model reproduced the decreasing trend and change of the slope due to the changed flow pattern at small openings but does not capture the slow recovery of C_Q at large openings. The positive slope was captured by the V2Fand k-ω-sst models, but much earlier (at Z/d0 = 0.05) than the experimental observation. The C_Q predicted by both models is more or less the same after this point. The C_Q computed by EB/Lag EB k-ε models converge once Z/d0 > 0.05.

Although the standard k-ε models poorly predict the trend of C_Q, it does reproduce the general ‘tick’ shape of C_F, as shown in Figure 13. That said there is a considerable quantitative discrepancy for small openings. Other models which predict the same tendency are the realizable k-ε models, and the k-ω-sst model, while others failed to capture any minimum at small openings. For small openings (Z/d0 < 0.05), the k-ω-sst model captures the minimum particularly well. It is also worth pointing out that an unexplained fluctuation exists near Z/d0 = 0.05 for both the V2F and k-ω-sst models and these models fail to capture the change in net force direction (C_F > 1) at large openings. Although, the error by the realizable k-ε model with two-layer wall treatment (~10%) is worse than the k-ω-sst model (~1%) at the two smallest openings, the former displays better performance across the full range of openings. The error in C_F obtained by the realizable k-ε model is within ±15%, while errors by other models can be in excess of ±20%.

The sensitivity due to different inlet flow profiles is presented in Figure 14. Compared to the conic valve, the variation of predicted valve performance due to the different inlet flow profiles is large. The effect is stronger for higher valve openings. As in the conic valve case, however, it is small compared to the modelling errors which are around ±10% to ±15%.

The Compensated Valve

As a result of the similarity of the valve head configuration to the conical valve, the first two flow patterns (I & II) in the conic valve study were also observed in the compensated valve case [31]. At large openings, the jet follows the shape of the valve plug until it meets the chamber wall (Type I). The jet tends to reattach to the valve seat at small openings (Type II). The flow patterns were most likely to transition at Z/d0 = 0.1. The transition in flow pattern introduces a discontinuity in the profile of C_Q and C_F, which is a particular characteristic of such designs. According to analogous factors found in the conical valve, this also results in a bi-stable condition in the compensated valve and the flow pattern is similarly historically dependent. In this regard, initialization conditions will affect the numerical reconstruction of the flow pattern. In addition to comparing the performance of the different turbulence models, the effects of the initialization conditions on the prediction of flow in the compensated valve are also be discussed below.

There are two initialization methods considered in the following discussions. One method is to initialize the flow domain with zero velocity and pressure, the other is to feed the flow domain with results from a simulation using the standard k-ε model with the standard wall function model, at the initialization step. For simplicity, these two methods will be termed as 'zero initialization' and 'std k-ε initialization' in the following discussions. The flow pattern around the plug at Z/d0 ≈ 0.1 obtained by the different turbulence models and the two initializing conditions are included in Table 3.

It is found that the impact of the initializing conditions varies between the different turbulence models, though no difference is seen between the versions of the standard k-ε and realizable k-ε and these are not included in the table. With the zero initialization conditions, Type II flow was predicted by the standard k-ε model as well as the Lag EB k-ε model, whereas Type I flow was shown in the simulation by other turbulence models. In the case of std k-ε initialization conditions, a Type I flow is preserved in predictions using the realizable k-ε and EB k-ε models, while the V2F and k-ω-sst model still generated a Type II flow. There is clearly a strong tendency for certain turbulence models to prefer one of these states, at least for this value of valve opening. The standard k-ε models tends to predict type II flows, whilst the V2F and k-ω-sst models are tend to predict type I flows. Only the realizable k-ε, the EB k-ε and the Lag EB k-ε models exhibit both types of flow depending on initializing condition. This behaviour is strongly dependent on the valve opening, as explained below, where the transition from type II to type I flows is considered in more detail.

The predicted initialization condition dependent valve performance parameters are depicted in Figure 15, whilst the related errors are included in Figure 16. The black symbols with dashed line in the figures are for the numerical results with the zero initialization conditions in the simulations, whilst the blue symbols and dashed line are predictions with std k-ε initialization in the models.

Regardless of the initialization conditions, the predicted discontinuities in profiles of C_Q and C_F do not match well with experimental observation, no matter what turbulence model was used. Furthermore, the errors between the predicted valve parameters and physical measurements are largest around the discontinuity. As illustrated in Figure 15, C_Q is overestimated whereas C_F was underestimated by the standard k-ε model, and the onset of the discontinuity in the C_Q and C_F profiles were greatly delayed for larger openings. The modified standard k-ε models (two-layer wall treatment or low-Re version) do not improve the predictions. In particular, the sudden change is not captured at all by the standard low-Re k-ε model within the opening range. In addition, the effects of initialization conditions on these k-ε type models are insignificant.

For the remaining five turbulence models, the occurrence of the discontinuity is generally only seen at smaller openings when applying the zero-initialization, rather than the std k-ε initialization. Other than the onset of the discontinuity in the profiles, the effects of the initialization conditions are negligible when applying the V2F and k-ω-sst models. For the analyses using the realizable k-ε model, EB k-ε model or lag EB k-ε model, the C_Q and C_F values predicted using the std k-ε initialization are normally smaller than those using the zero initialization. Such differences are more obvious in the prediction of C_F. Considering the discontinuity location predicted by the turbulence model with two initialization conditions, the realizable k-ε models and EB k-ε model is better than others. In terms of error ranges for C_Q, the performance of different turbulence models are broadly similar. As is presented in Figure 16, the errors in C_Q away from the onset of the discontinuity are generally within the range of ±5%, while the errors around the discontinuity point are about 6.5%, except for the prediction by standard k-ε models (>10%). For C_F, all CFD models tend to underestimate the value except for the realizable k-ε models. Away from the discontinuity, the errors in C_F are within the range of ±15% and ~20% around the discontinuity point.

The sensitivity of the numerical results to different inlet flow profiles at three valve openings are documented in Figure 17. As with the other cases, two factors are revealed: Firstly, the entry effect is insignificant in the considered opening range. The largest variations of predicted C_F and C_Q are just ~0.6%, which is ignorable in comparison with modelling errors and uncertainties due to different initializing conditions. Secondly the variations due to the development of the entry flow generally increase as the valve opening becomes larger.

Impacts of Non-linear Modifications and the Curvature Correction

As discussed in previous sections, the strong secondary recirculation, streamline curvature or even non-equilibrium conditions are expected in valve flows. This section is contributed to discuss predictions of valve flows due to non-linear modifications of the standard k-ε model (std k-ε (Quadratic) model and std k-ε (Cubic) model) and the k-ω-sst model (k-ω-sst (Quadratic) model and k-ω-sst (Cubic) model) as well as the curvature correction in the realizable k-ε model (realizable k-ε (Curv) model). The C_Q of the conical valve and the disk valve predicted by modified turbulence models as well as their standard versions are discussed. The numerical results of the conical valve are illustrated in Figure 18 while the results of the disk valve are included in Figure 19.

It is clearly presented in Figure 18 that only the C_Q predicted by non-linear modifications of the standard k-ε model shows visible differences in comparison with its standard version. Whilst the std k-ε (Quadratic) model shows similar predictions as the std k-ε model, the std k-

ε (Cubic) model makes the prediction worse. The predictions of C_Q by the realizable k-ε (Curv) model, k-ω-sst (Quadratic) model and k-ω-sst (Cubic) model almost overlap with the output of their standard counterparts.

Since stronger flow recirculation and stream curvature exit in the disk valve flow, impacts of turbulence model modifications are expected to be stronger. As shown in Figure 19, non-linear modifications of the standard k-ε model outperform its standard version in terms of both measures, namely trend and accuracy. While the opposite trend of C_Q was predicted by the standard k-ε model, the trend of C_Q by the std k-ε (Quadratic) model and std k-ε (Cubic) model follows the observation in the experiment. Thanks to non-linear modifications, errors were narrowed down, from [~-18%, ~20%] to [~-12%, ~2%]. It is also shown in the figure that the std k-ε (Quadratic) model is marginally better than the std k-ε (Cubic) model. Results of the realizable k-ε (Curv) model and non-linear versions of the k-ω-sst models exhibit visible differences in comparison with their standard versions. The curvature correction in the realizable k-ε makes the prediction ~5% worse in general. Except for the C_Q at Z/d0 = 0.0326, the change of the prediction due to the nonlinear modification of the k-ω-sst models (within $\pm 1.5\%$) is marginal compared to the errors.

Conclusions

This paper investigates the performance of several eddy viscosity models available in the STAR-CCM+ 12.04 regarding the prediction of the valve performance parameters, flow coefficient (C_Q) and force coefficient (C_F) of three types of valves. The main conclusions are as follows:

- The accuracy of the numerical predictions of both parameters indicates the capability of turbulence models to reproduce the general flow topologies in the valve. The performance of eddy viscosity models varies in predictions of different valve flows.
    - For the conic valve, the performance of the turbulence models show relatively modest variation and are quite consistent. The standard k-ε model is marginally better than others, except for the very small opening.
    - For the disk valve, the turbulence models perform differently in terms of predicting C_Q and C_F. It is clear that the realizable k-ε model (standard version) outperformed others in terms of prediction C_Q, while the standard k-ε model (standard version) does not even capture the correct trend. Considering the prediction of C_F, the realizable k-ε model (standard version) is better than others when the lift of the valve is small. But the standard k-ε model (standard version) and Lag EB k-ε model outperformed the realizable k-ε model as $z/d0 \geq 0.07$.
    - For the compensated valve, the performance of the standard k-ε model (standard version) is the poorest compared to other considered models. The realizable k-ε model and EB k-ε model outperformed others as they can provide better predictions of the discontinuity locations in the profiles, no matter what initialization conditions were applied. Their predictions also show smaller errors.
- Errors of predicted C_F are generally higher than the C_Q for all turbulence models. One of the possible explanations is that the error cancelling is more likely to happen in the

calculation of the C_Q. Since the C_Q is calculated by the pressure difference at locations away from the throttle while the C_F is evaluated according to the pressure around the valve head.

- The two-layer & low-Re versions of the standard k-ε model do not improve the prediction although such modifications tend to improve the prediction of the near wall flow. The realizable k-ε model benefits from improved numerical stability when the standard wall function is employed.
- Once the strong circulation and/or streamline curvature are expected in the flow, such as disk valve flow, non-linear modifications of the standard k-ε model will greatly improve predictions of the flow coefficient. Meanwhile, the curvature correction of the realizable k-ε model presents minor (in the case of the conical valve) or negative (in the case of the disk valve) effects on the accuracy. The impact of non-linear modifications of the k-ω-sst model is minor.
- If multiple stable flow states exist in the flow domain, as seen in the compensated valve, the predictions of the model may converge to different stable states according to the initialization condition, which will also change the predicted valve performance parameters.
- Finally, the variation of the numerical results due to the unknown development stage of the entry flow is small in our study. However, in practice, its value may be comparable to the general modelling error.

Acknowledgements

The authors would like to thank Rolls-Royce for the financial and moral support that made this work possible.

Nomenclature

a	orifice of the valve
d_{in}, d0	diameter of inlet pipe
d_{out}	diameter of chamber
k	turbulent kinetic energy
sst	shear stress transport
A	area of inlet pipe
C_F	force coefficient
C_Q	flow coefficient
C_v	discharge coefficient
CFD	Computational Fluid Dynamics
EB	Elliptic Blending
F	force on the plug
Q	volumetric flow rate
RANS	Reynolds-Averaged Navier-Stokes equations
Re	Reynolds number
RNG	Re-Normalisation Group
std	Standard
Z	lift of the plug
ε	turbulent dissipation rate
ρ	density
ω	specific dissipation rate
θ	half angle of poppet cone
ΔP	pressure drop across the valve

REFERENCES

1. Song, X. G., Cui, L. & Park, Y. C. Three-dimensional CFD analysis of a spring-loaded pressure safety valve from opening to re-closure. in the ASME 2010 Pressure Vessels & Piping Division / K-PVP Conference 1–9 (2010).

2. Song, X. G., Kim, S. G., Wang, L. & Park, Y. C. Transient Flow analysis of spring loaded pressure safety valve. in the ASME 2009 Pressure Vessels and Piping Division Conference 1–6 (2009).

3. Song, X. G., Park, Y. C. & Park, J. H. Blowdown prediction of a conventional pressure relief valve with a simplified dynamic model. Math. Comput. Model. 57, 279–288 (2013).

4. Song, X. et al. A CFD analysis of the dynamics of a direct-operated safety relief valve mounted on a pressure vessel. Energy Convers. Manag. 81, 407–419 (2014).

5. Lisowski, E. & Rajda, J. CFD analysis of pressure loss during flow by hydraulic directional control valve constructed from logic valves. Energy Convers. Manag. 65, 285–291 (2013).

6. Lisowski, E., Czyzycki, W. & Rajda, J. Three dimensional CFD analysis and experimental test of flow force acting on the spool of solenoid operated directional control valve. Energy Convers. Manag. 70, 220–229 (2013).

7. Jin, Z.-J., Wei, L., Chen, L.-L., Qian, J.-Y. & Zhang, M. Numerical simulation and structure improvement of double throttling in a high parameter pressure reducing valve. J. Zhejiang Univ. Sci. A 14, 137–146 (2013).

8. Chern, M., Hsu, P., Cheng, Y., Tseng, P. & Hu, C. Numerical Study on Cavitation Occurrence in Globe Valve. J. Energy Eng. ASME 139, 25–34 (2013).

9. Chern, M.-J. et al. Design of cages in globe valve. Proc. Inst. Mech. Eng. Part C J. Mech. Eng. Sci. 229, 476–484 (2015).

10. Velusamy, K. et al. Computational fluid dynamic investigations and experimental validation of frozen seal sodium valve assembly of a fast reactor. Ann. Nucl. Energy 37, 1423–1434 (2010).

11. Yang, S. D., Kim, C. K., Jeon, S. Y. & Yoon, J. Y. Numerical performance and safety analyses of a retainer-type ball valve for use in a high-pressure district heating pipeline. Proc. Inst. Mech. Eng. Part E J. Process Mech. Eng. 0, 1–12 (2016).

12. Whitehead, N. P., Slaouti, A. & Taylor, H. Optimisation of Flow Through a Pneumatic Control Valve using CFD Analysis and Experimental Validation. 9776, (2017).

13. Jin, Z., Gao, Z., Zhang, M. & Qian, J. Pressure Drop Analysis of Pilot-Control Globe Valve With Different Structural Parameters. J. Fluids Eng. 139, 91102 (2017).

14. Jin, Z., Gao, Z., Zhang, M. & Liu, B. Computational fluid dynamics analysis on orifice structure inside valve core of pilot-control angle globe valve. in IMechE Part C: J Mechanical Engineering Science 0, 1–11 (2017).

15. Chern, M.-J. & Wang, C.-C. Control of Volumetric Flow-Rate of Ball Valve Using V-Port. J. Fluids Eng. 126, 471 (2004).

16. CD-adapco, STAR-CCM+ Documentation, version 12.04.

17. Vaughn, N. D., Johnston, D. N. & Edge, K. A. Numerical Simulation of Fluid Flow in Poppet Valves. Proc. Inst. Mech. Eng. Part C J. Mech. Eng. Sci. 206, 119–127 (1992).

18. Huang, C. & Kim, R. H. Three-Dimensional Analysis of Partially Open Butterfly Valve Flows. J. Fluids Eng. 118, 562 (1996).

19. Wallace, M. S., Dempster, W. M., Scanlon, T., Peters, J. & McCulloch, S. Prediction of impact erosion in valve geometries. Wear 256, 927–936 (2004).

20. Song, X. & Park, Y. C. Numerical Analysis of Butterfly Valve-Prediction of Flow Coefficient and Hydrodynamic Torque Coefficient. in Proceedings of the World Congress on Engineering and Computer Science 2007 2–6 (2007). doi:978-988-98671-6-4

21. Palau-Salvador, G., González-Altozano, P. & Arviza-Valverde, J. Three-Dimensional Modeling and Geometrical Influence on the Hydraulic Performance of a Control Valve. J. Fluids Eng. 130, 11102 (2008).

22. Davis, J. A. & Stewart, M. Predicting Globe Control Valve Performance—Part I: CFD Modeling. J. Fluids Eng. 124, 772 (2002).

23. Davis, J. A. & Stewart, M. Predicting globe control valve performance—Part II: Experimental verification. J. Fluids Eng. 124, 778–783 (2002).

24. Moujaes, S. F. & Jagan, R. 3D CFD Predictions and Experimental Comparisons of Pressure Drop in a Ball Valve at Different Partial Openings in Turbulent Flow. J. Energy Eng. 134, 24–28 (2008).

25. Sibilla, S. & Gallati, M. Hydrodynamic Characterization of a Nozzle Check Valve by Numerical Simulation. J. Fluids Eng. 130, 121101 (2008).

26. Toro, A. D. MSc Thesis, Computational Fluid Dynamics Analysis of Butterfly Valve Performance Parameters. (2012).

27. Leutwyler, Z. & Dalton, C. A CFD study to analyze the Aerodynamic torque, lift and drag forces for a butterfly valve in the mid-stroke position. in ASME Heat Transfer/Fluids Engineering Summer Conference 1–9 (2004).

28. Leutwyler, Z. & Dalton, C. A Computational Study of Torque and Forces Due to Compressible Flow on a Butterfly Valve Disk in Mid-stroke Position. J. Fluids Eng. 128, 1074 (2006).

29. Simic, M. & Herakovic, N. Reduction of the flow forces in a small hydraulic seat valve as alternative approach to improve the valve characteristics. Energy Convers. Manag. 89, 708–718 (2015).

30. Menter, F. R. Review of the shear-stress transport turbulence model experience from an industrial perspective. Int. J. Comut. Fluid Dyn. 23, 305–316 (2009).

31. Johnston, D. N., Edge, K. a & Vaughan, N. D. Experimental investigation of flow and force characteristics of hydraulic poppet and disc valves. Arch. Proc. Inst. Mech. Eng. Part A J. Power Energy 205, 161–171 (1991).

Table 1: Mesh configurations of 45˚ conical valve.

Msh	V1	H1	V2	H2	V3	H3	V4	H4
1	10	50	20	20	30	130	30	30
2			30	30				
3			60	60				
4			300	300				
5	60					180		
5a	60							
6	50					170		
7	40					160		
8	30					150		
9	30		40	30		140		
9a	30					140		

Table 2: Maximum y+ values in meshes

Msh	Inlet Pipe	Chamber	VH-Frnt	SPND	Guide
1	17	34	29	4	12
2					
3					
4					
5	3.6	33.6	6.3	4	11.6
5a	1.23	0.5	1.1	0.6	0.2
6	5.6	33.5	7.15	4	11.6
7	6.2	33.6	8.53	4	11.6
8	7.7	33.6	10.6	4	11.6
9	7.7	33.6	10.6	4	11.6
9a	1.64	0.45	0.17	1.16	0.19

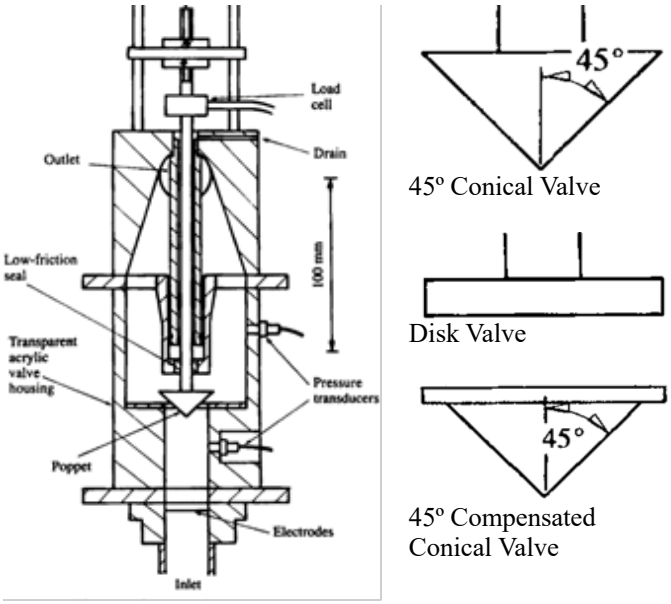


Figure 1: A schematic view of the experimental rig by Johnston, Edge & Vaughan [31].

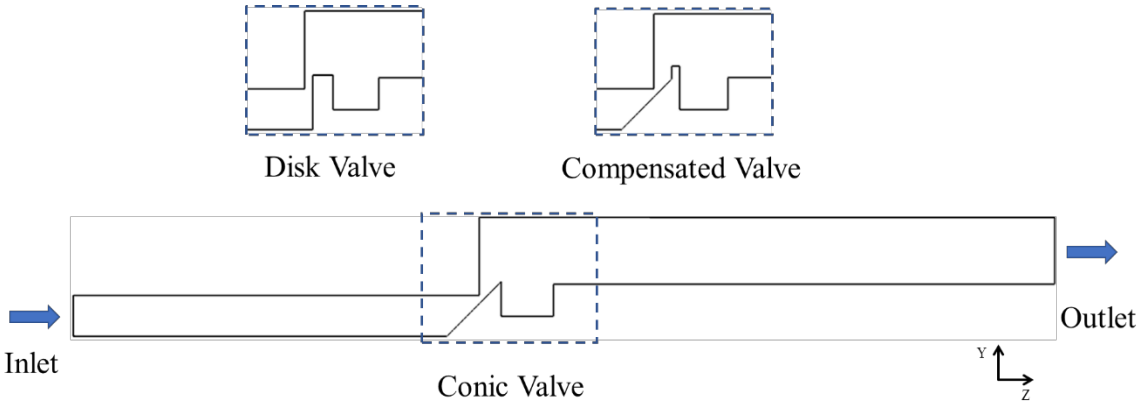


Figure 2: Considered geometries in the CFD models

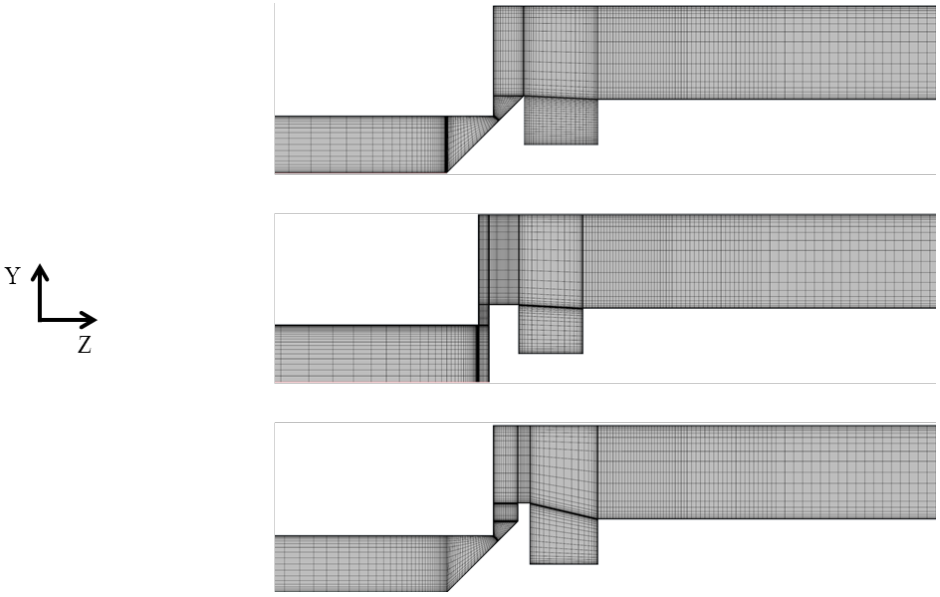


Figure 3: A view of the meshes of the studied valves.

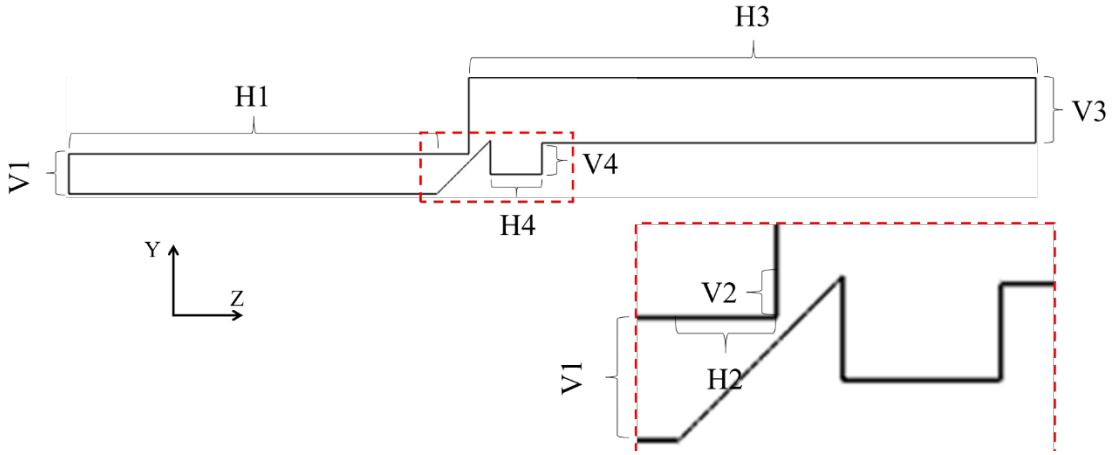


Figure 4: Edges of the conic valve.

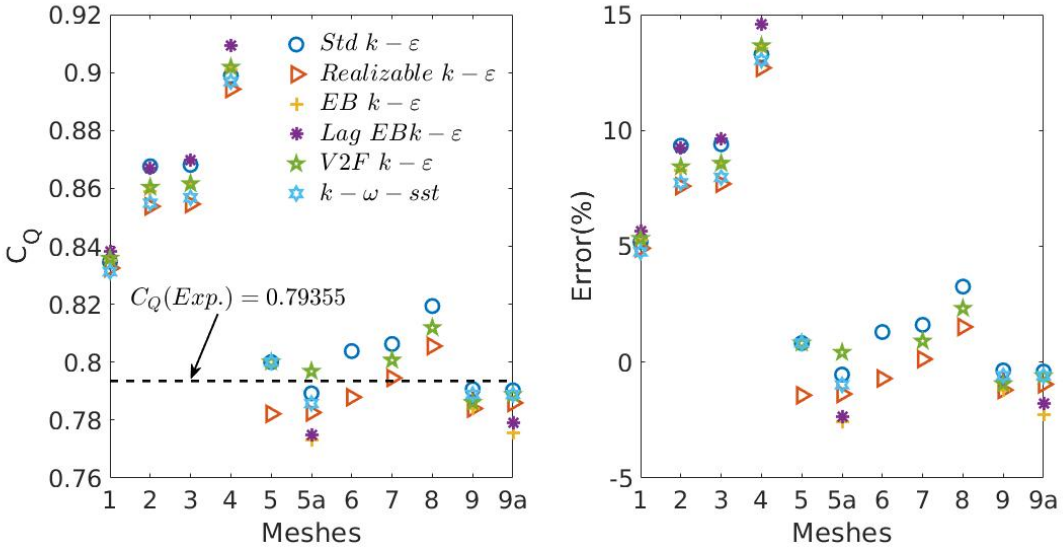


Figure 5: The C_Q of the conical valve measured by experiment and predicted by CFD models with various eddy viscosity models and different meshes in the case of 2.54 mm lift.

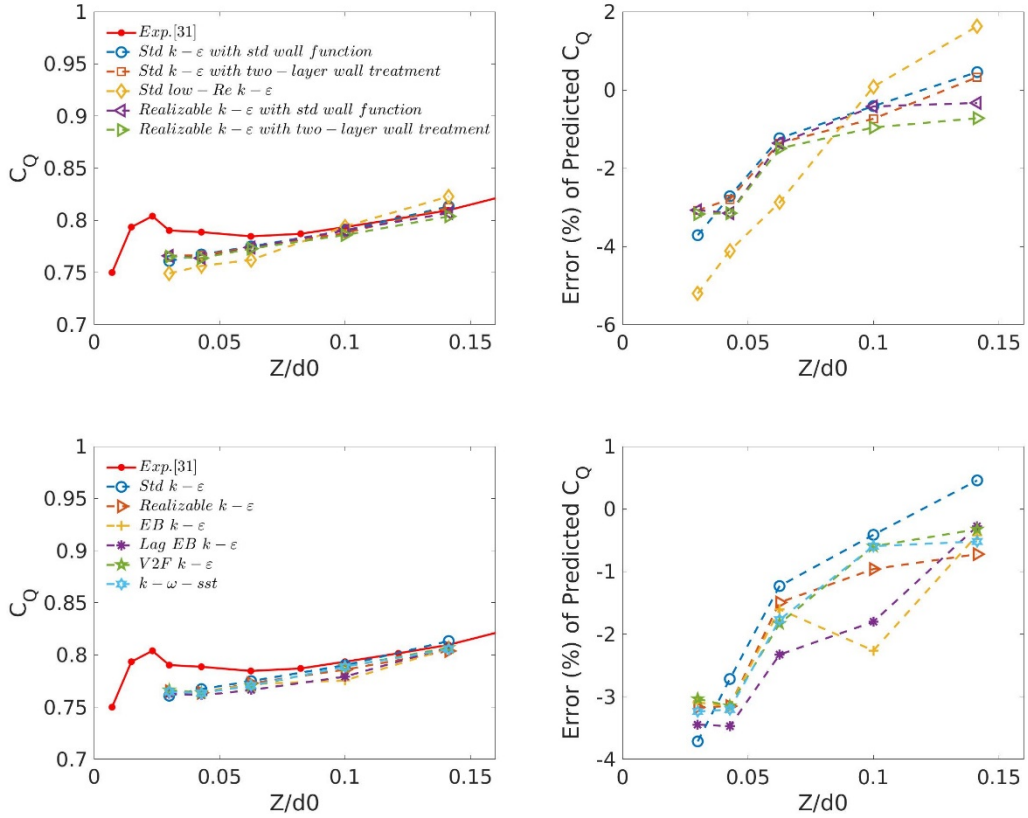


Figure 6: The C_Q of the conical valve measured in the experiments and predicted by CFD models using different turbulence models.

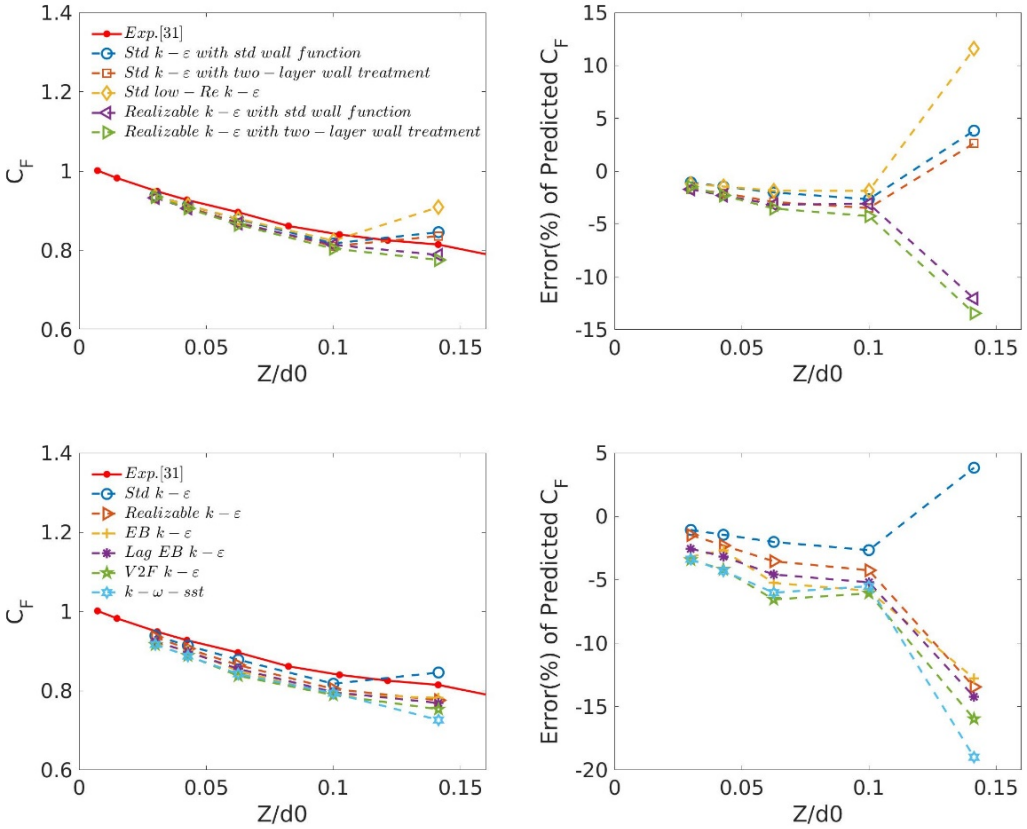


Figure 7: The C_F of the conical valve measured in the experiments and predicted by CFD models using different turbulence models.

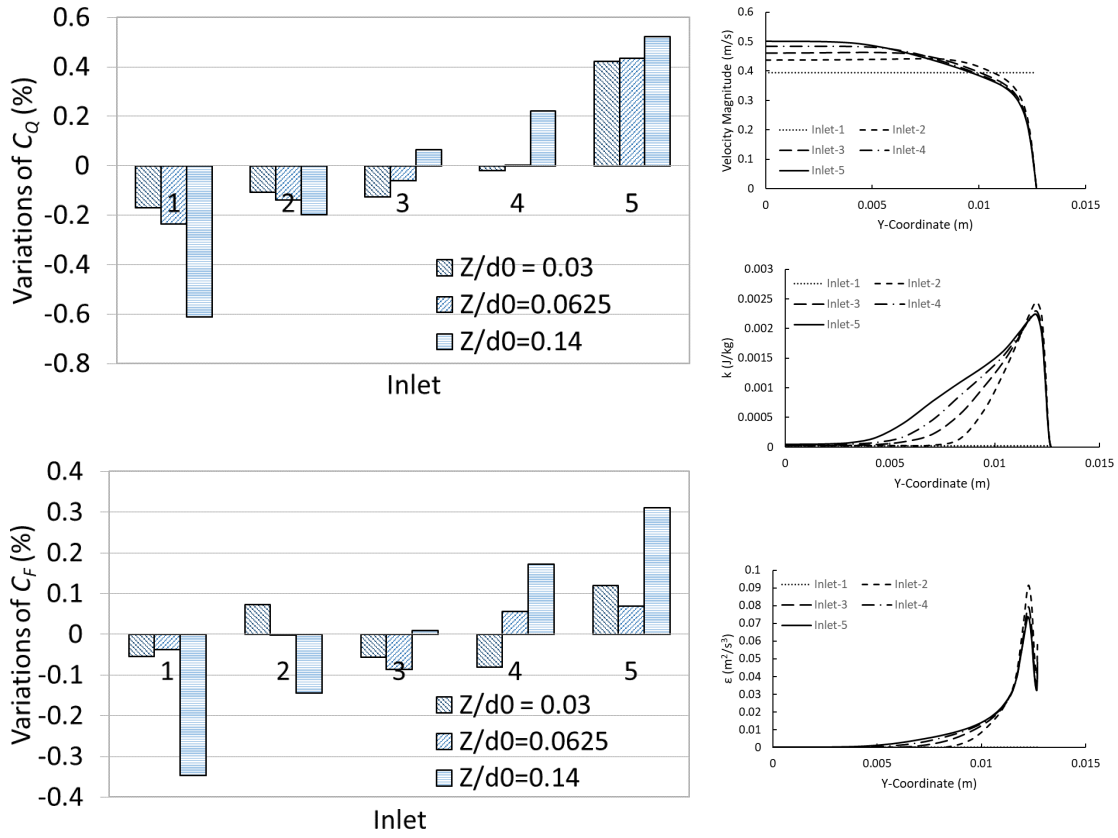


Figure 8: Variations of predicted C_Q and C_F of a conical valve due to different inlet flow conditions.

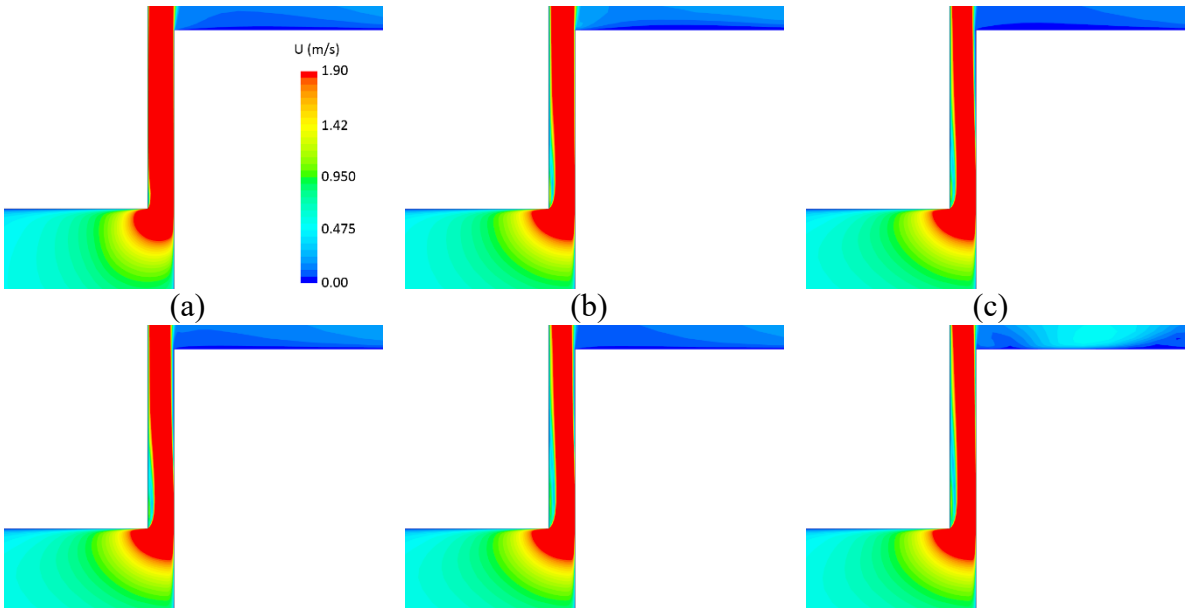


Figure 9: Flow pattern around the clearance formed by disk valve head and valve seat at z/d0=0.025 predicted by (a) standard k-ε model with high y^+ wall treatment; (b) realizable k-ε model with two-layer wall treatment; (c) EB k-ε model; (d) Lag EB k-ε model; (e) V2F model; (f) k-ω-sst model.

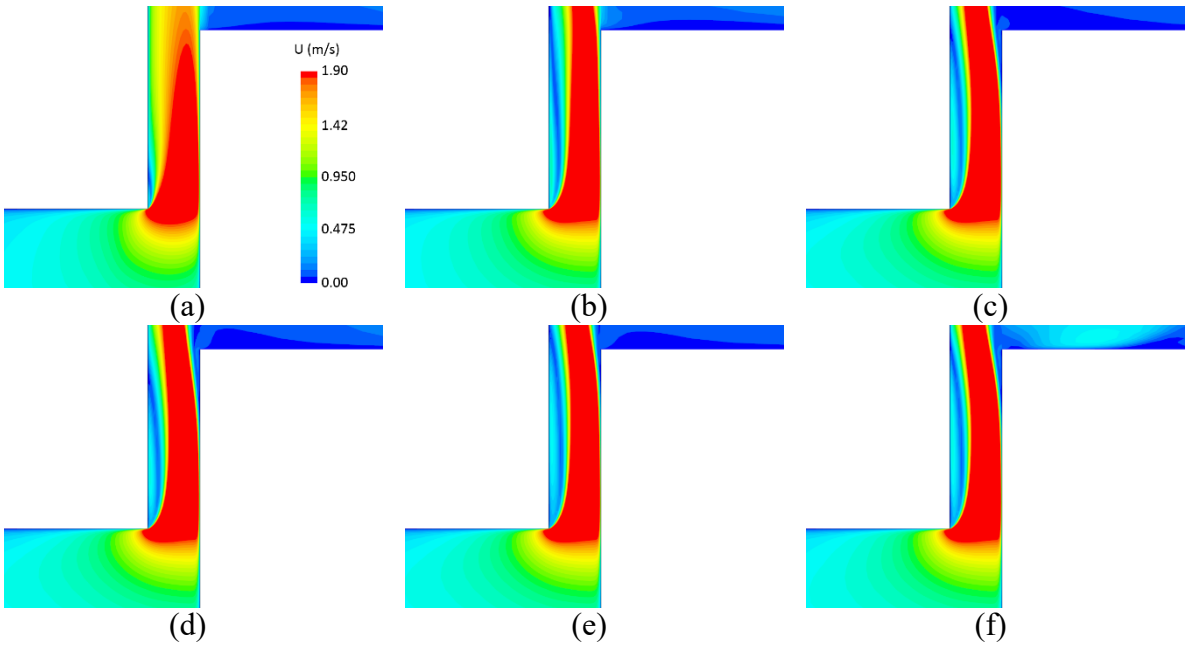


Figure 10: Flow pattern around the clearance formed by disk valve head and valve seat at z/d0=0.05 predicted by (a) standard k-ε model with high y^+ wall treatment; (b) realizable k-ε model with two-layer wall treatment; (c) EB k-ε model; (d) Lag EB k-ε model; (e) V2F model; (f) k-ω-sst model.

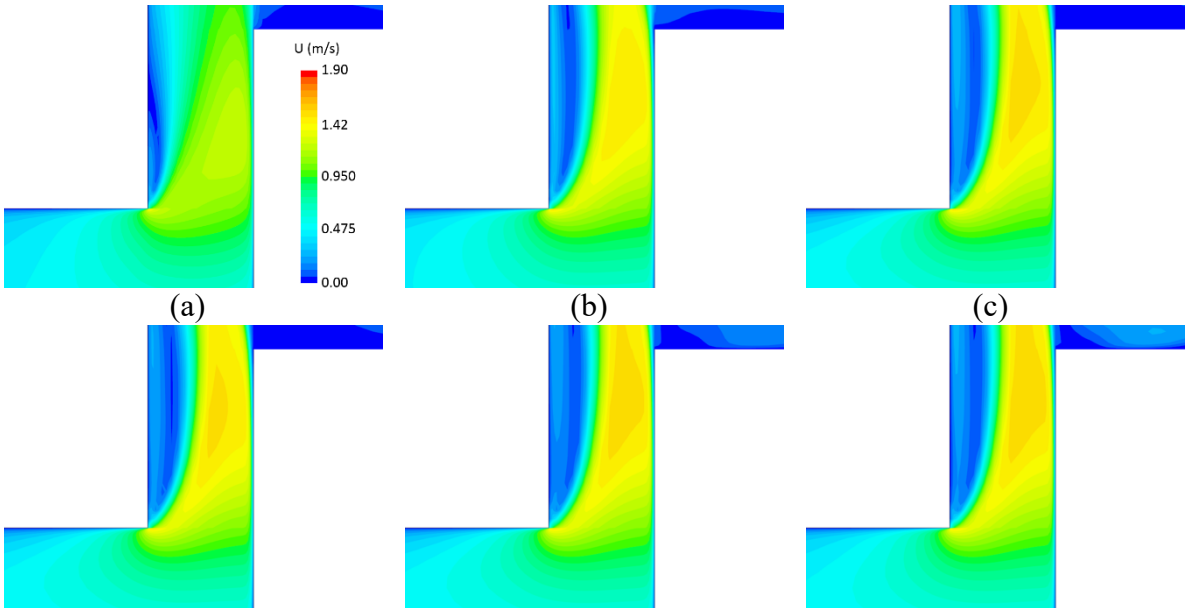


Figure 11: Flow pattern around the clearance formed by disk valve head and valve seat at z/d0=0.1 predicted by (a) standard k-ε model with high y^+ wall treatment; (b) realizable k-ε model with two-layer wall treatment (c) EB k-ε model; (d) Lag EB k-ε model; (e) V2F model; (f) k-ω-sst model.

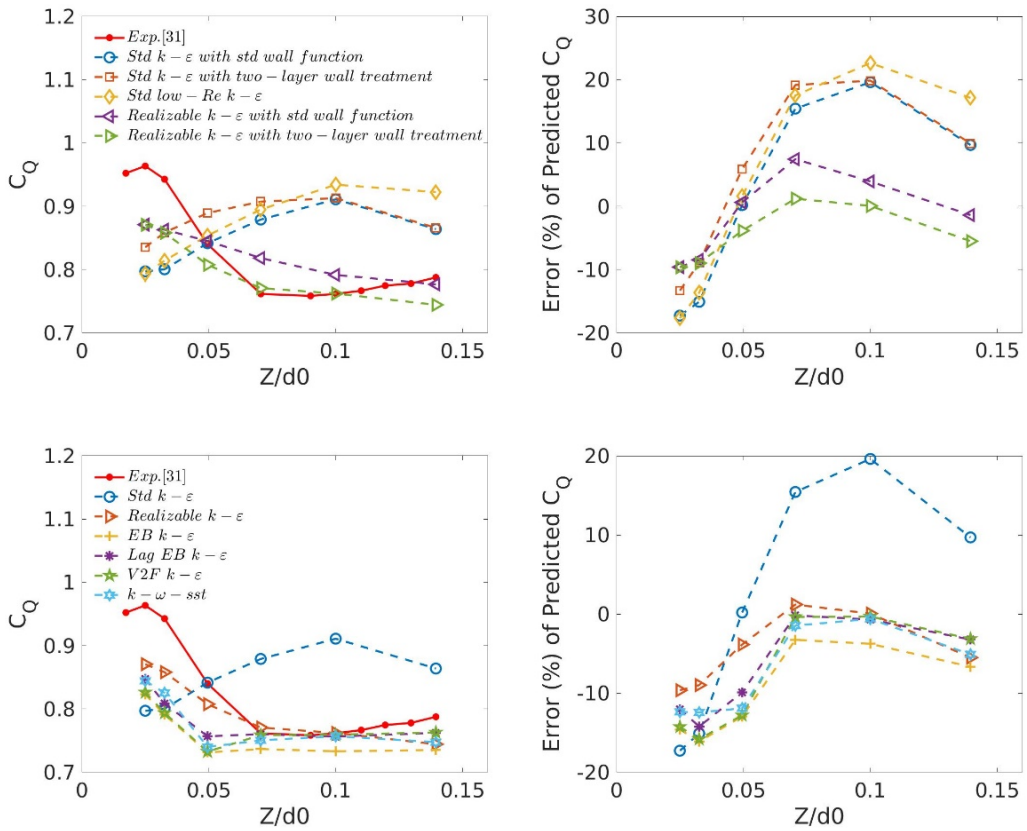


Figure 12: The C_Q of the disk valve measured in the experiments and predicted by CFD models using different turbulence models.

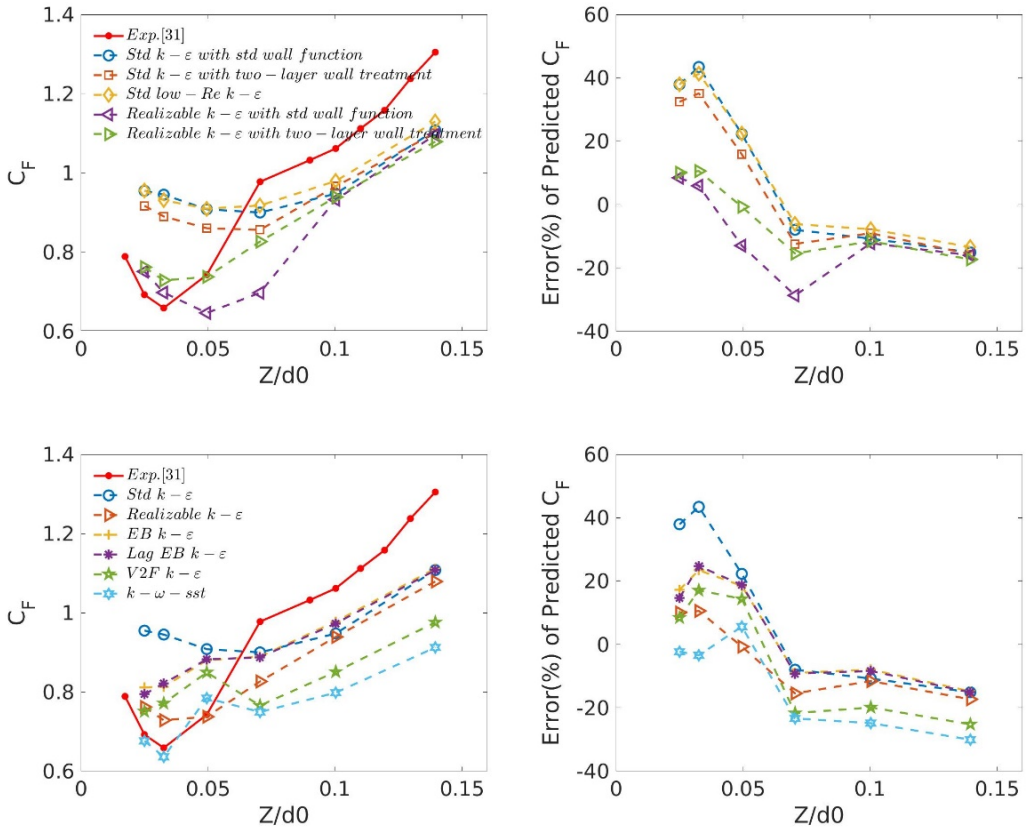


Figure 13: The C_F of the disk valve measured in the experiments and predicted by CFD models using different turbulence models.

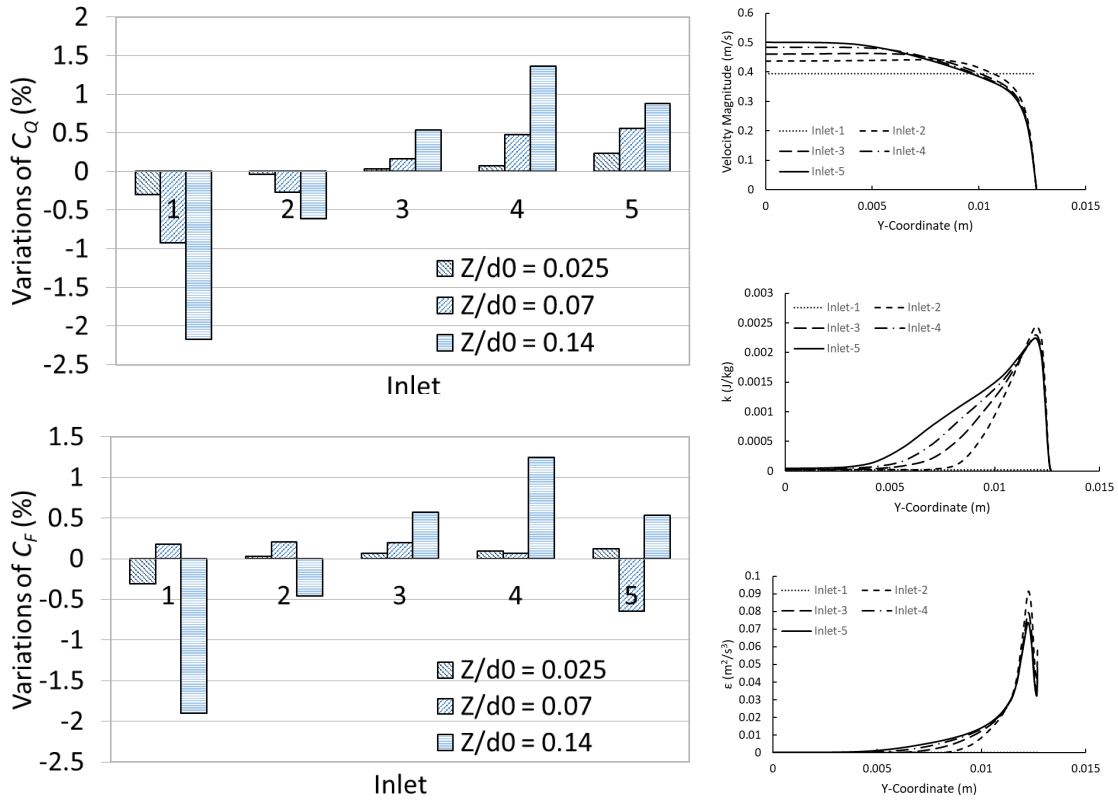
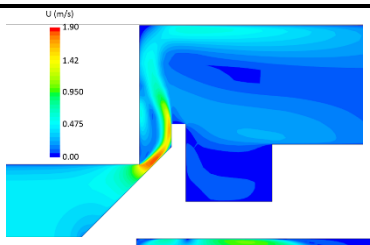
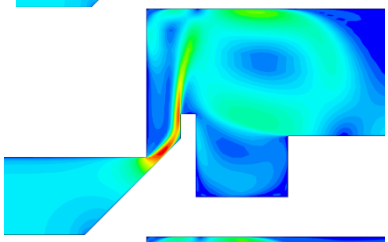
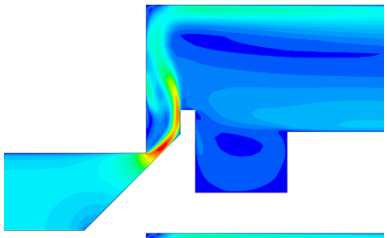
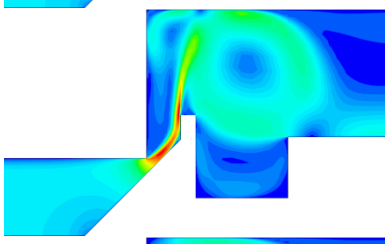
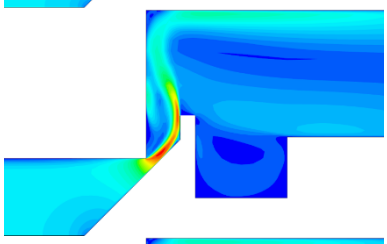
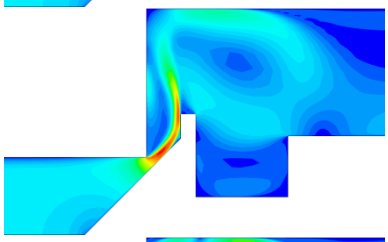
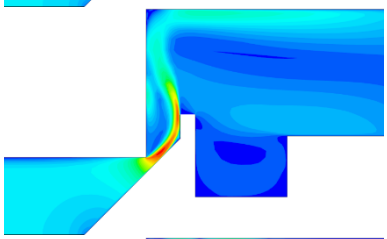
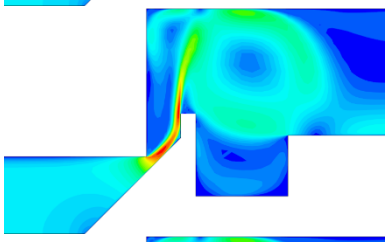
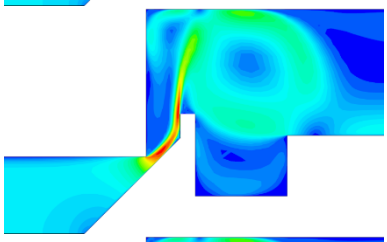
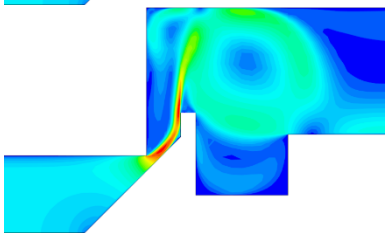
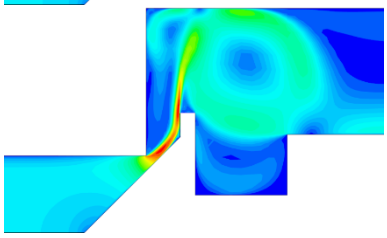
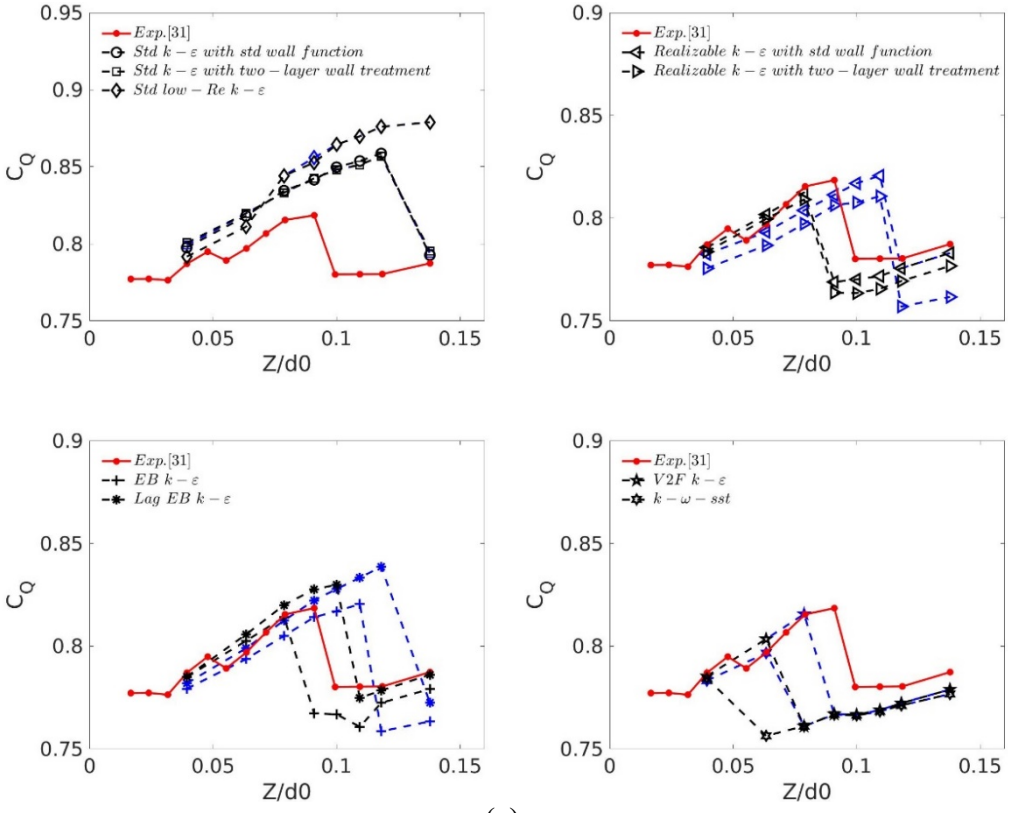


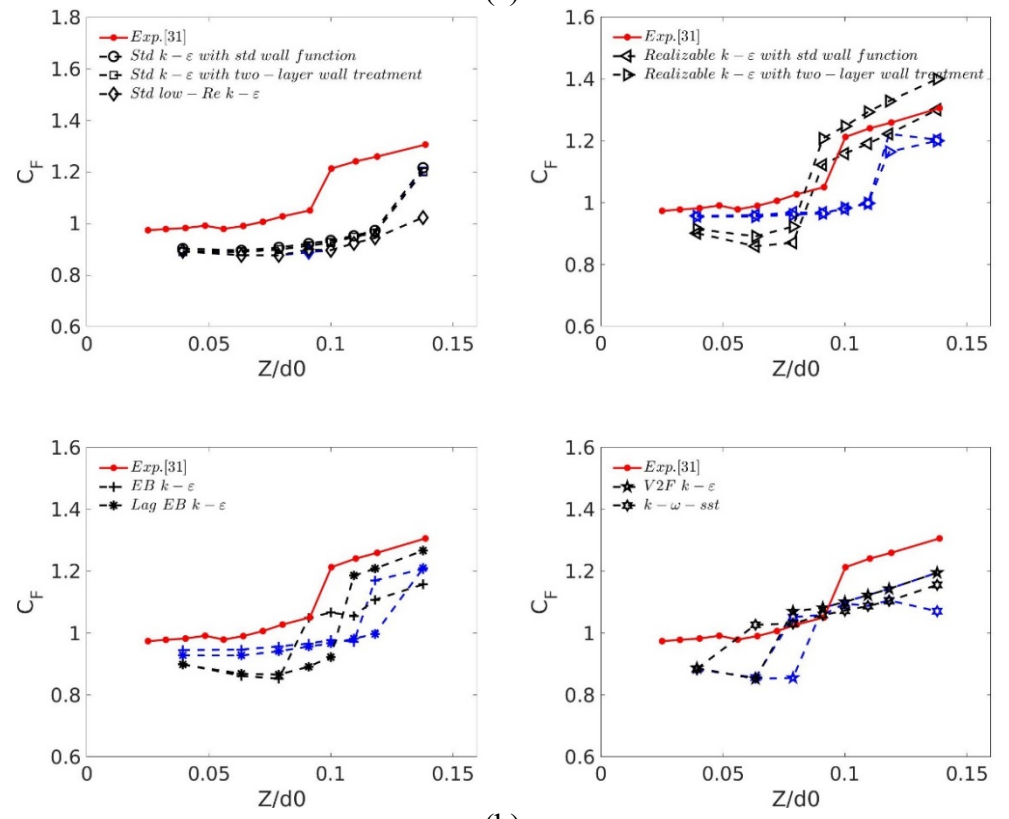
Figure 14: Variations of predicted C_Q and C_F of disk valve due to different inlet flow conditions.

Table 3: The flow domain around the compensated valve head at Z/d0 ≈ 0.1 predicted using different turbulence modelling methodologies regarding two different initialization conditions.

Turbulence model & near wall flow treatment	Initialized by	
	Zeros	Results of standard k-ε
Standard k-ε model		
Realizable k-ε model		
EB k-ε model		
Lag EB k-ε model		
V2F model		
k-ω-sst model		

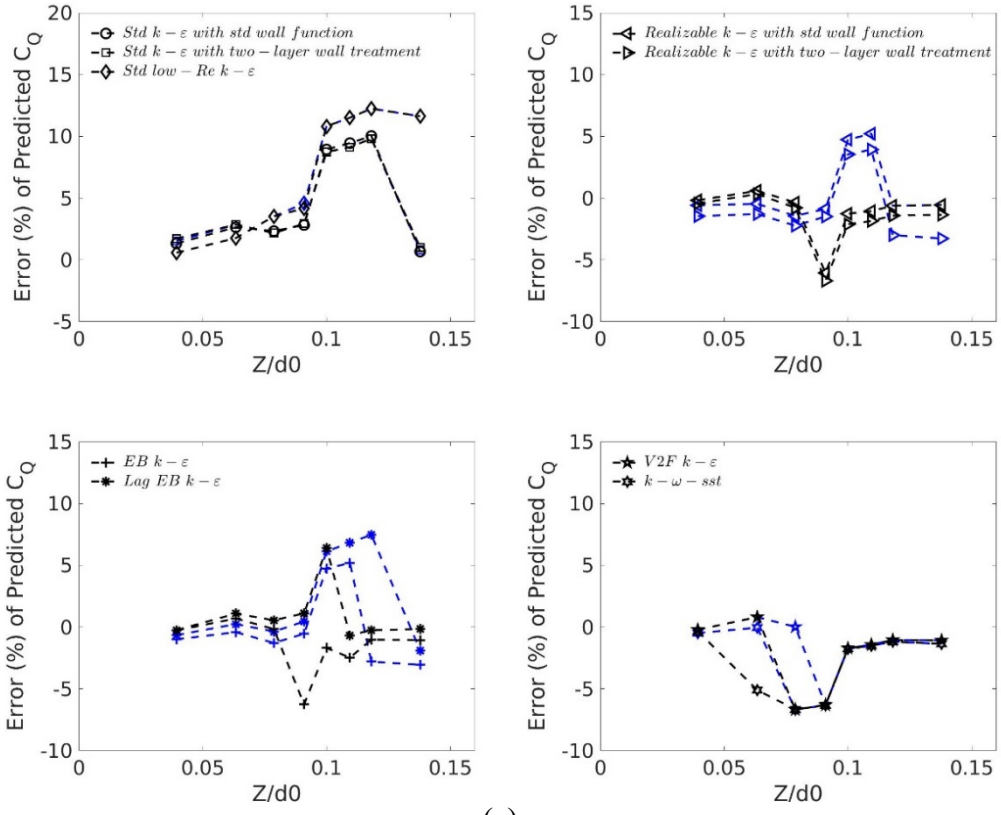


(a)

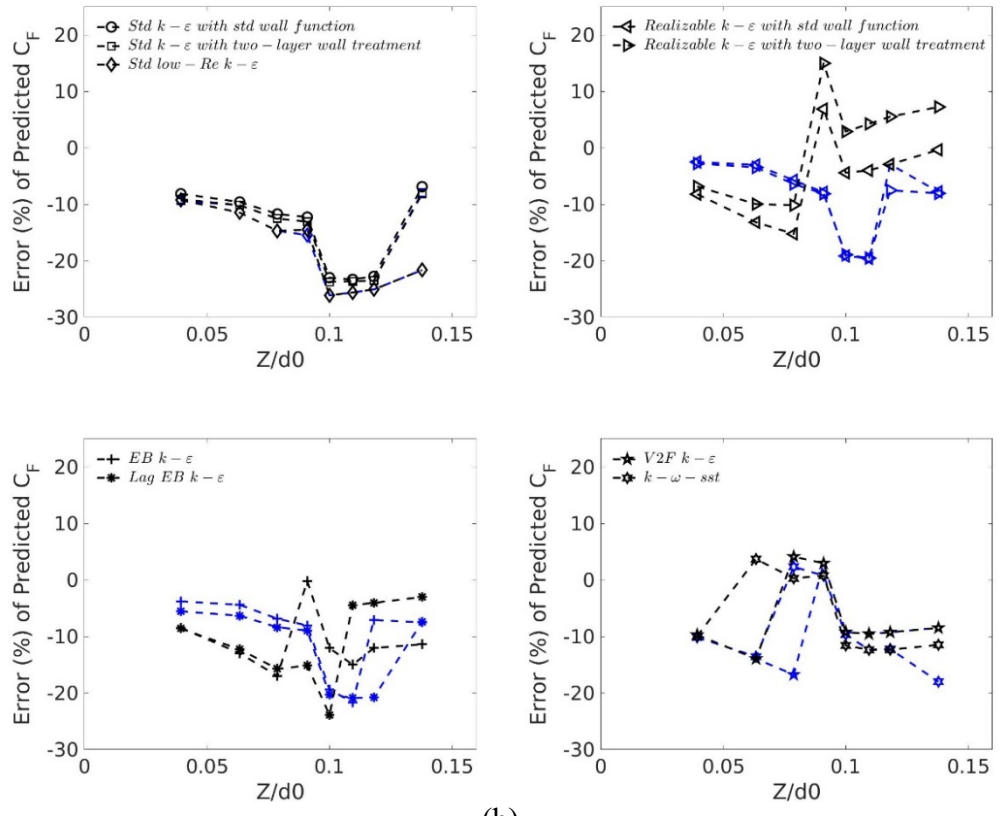


(b)

Figure 15: The valve parameter (a) C_Q; (b) C_F measured in the experiments and predicted by CFD models using different turbulence models and initial conditions. The dark dashed line and symbols are predictions using zero velocities and pressure as initial conditions. The blue dashed line and symbols are predictions using results of standard k-ε model as initial conditions.



(a)



(b)

Figure 16: Errors of predicted valve parameters (a) C_Q, (b) C_F of compensated valve. The dark dashed line and symbols are predictions using zero velocities and pressure as initial conditions. The blue dashed line and symbols are predictions using results of standard k-ε model as initial conditions.

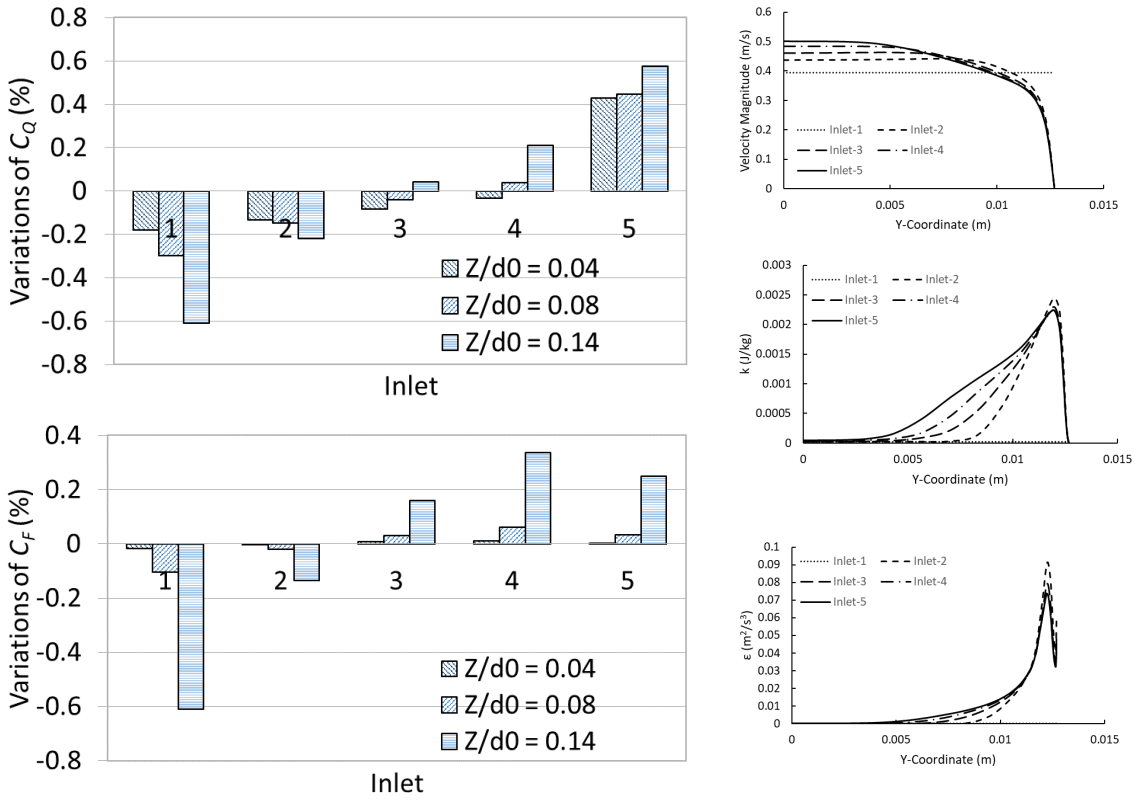


Figure 17: Variations of predicted C_Q and C_F of compensated poppet valve due to inlet flow conditions.

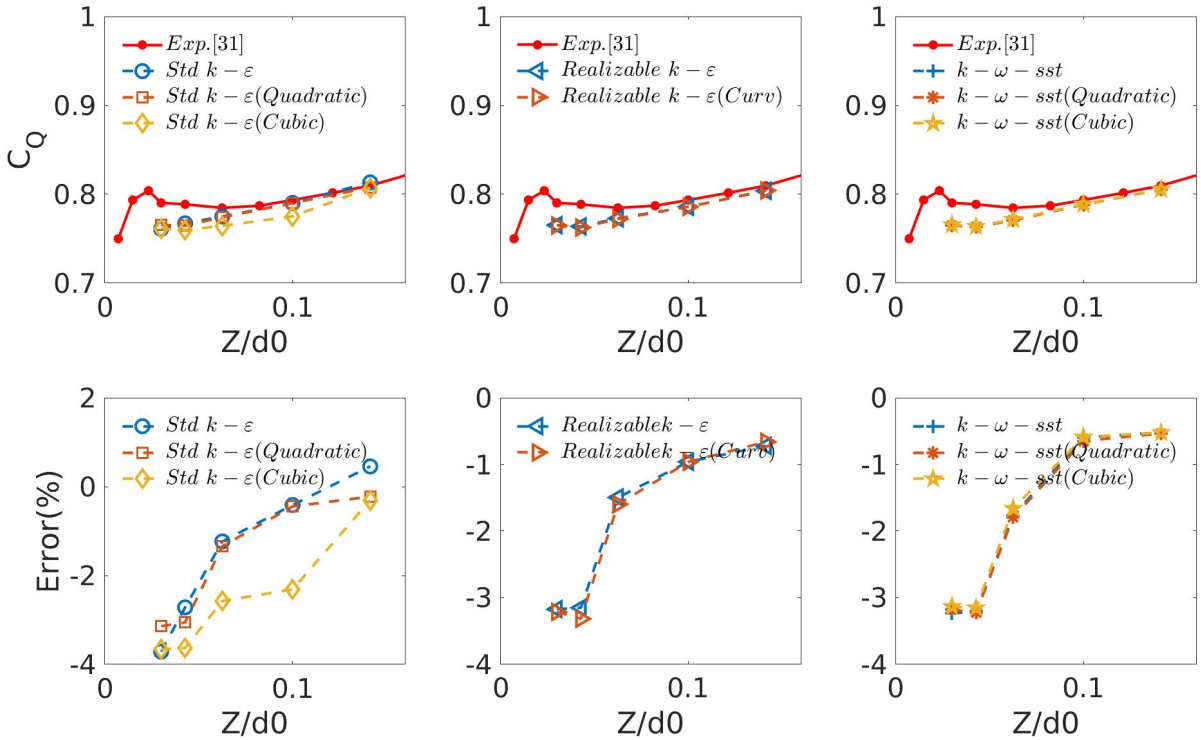


Figure 18: Comparison of C_Q of the conical valve predicted by nonlinear versions of the standard k-ε model and the k-ω-sst model and the curvature correction version of the realizable k-ε model with the outputs from their standard versions.

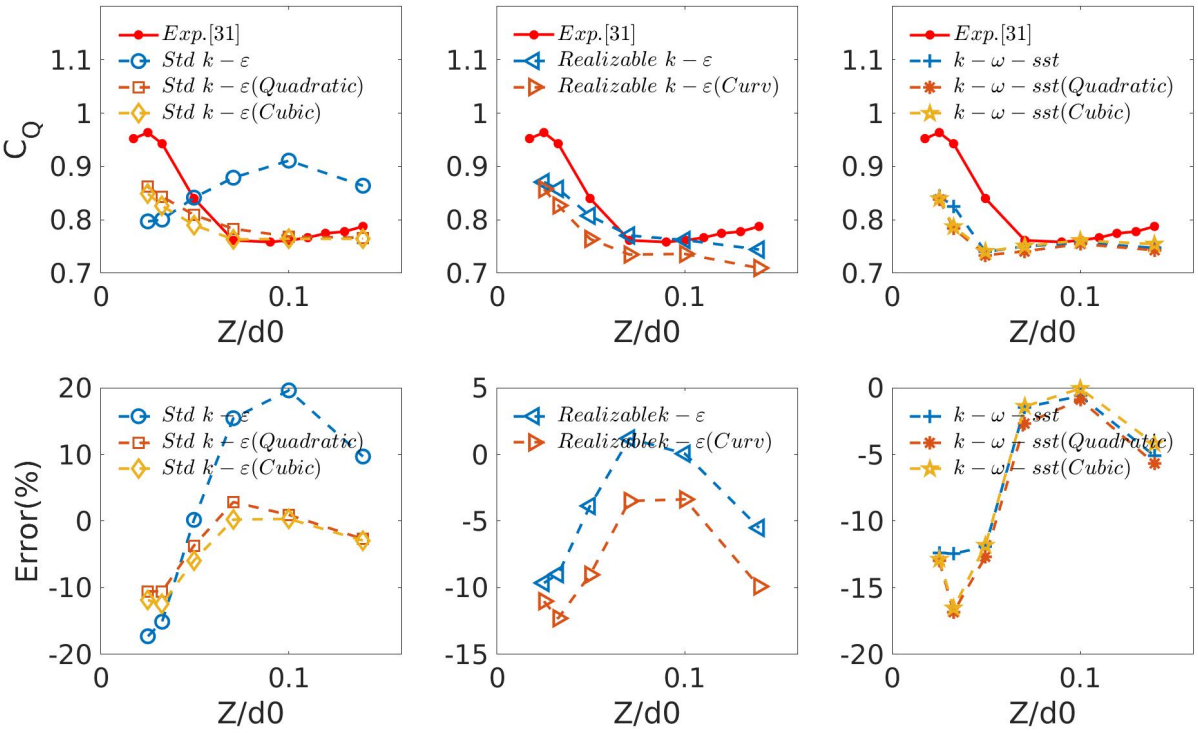


Figure 19: Comparison of C_Q of the disk valve predicted by nonlinear versions of the standard k-ε model and the k-ω-sst model and the curvature correction version of the realizable k-ε model with the outputs from their standard versions.